Correlation function for the $n\bar{D}^*_{s0}(2317)$ interaction and the issue of elastic unitarity

Natsumi Ikeno (Kobe University)

Eulogio Oset (University of Valencia–IFIC)

N. Ikeno and E. Oset, Phys. Rev. D **112**, 094019 (2025)

ETHNP (Effective Theories in Hadron and Nuclear Physics) workshop

September 3th to 5th, 2026, Valencia

Correlation Functions in Hadron Physics

Femtoscopy: a powerful tool to probe hadron interactions via two-particle correlation functions

For a review, see: L. Fabbietti, V. Mantovani Sarti, O. Vazquez Doce, Ann. Rev. Nucl. Part. Sci. **71**, 377 (2021)

- Correlation functions (CFs), together with spectroscopy, provide information on hadron dynamics
- Especially powerful for pairs **inaccessible in scattering experiments**
- Recently extended to **three-body** correlations

Numerous theoretical studies:

- A. Ohnishi, K. Morita, K. Miyahara, T. Hyodo, NPA 954, 294 (2016)
- Y. Kamiya, T. Hyodo, K. Morita, A. Ohnishi, W. Weise, PRL124, 132501 (2020)
- Z. W. Liu, J. X. Lu and L. S. Geng, PRD **107**, 074019 (2023)
- I. Vidana, A. Feijoo, M. Albaladejo, J. Nieves and E. Oset, PLB **846**, 138201 (2023)
- N. Ikeno, G. Toledo and E. Oset, PLB **847**, 138281 (2023)
- R. Molina, C. W. Xiao, W. H. Liang and E. Oset, PRD **109**, 054002 (2024)
- K. P. Khemchandani, L. M. Abreu, A. Martinez Torres and F. S. Navarra, PRD **110**, 036008 (2024)
- P. Encarnación, A. Feijoo, V. M. Sarti and A. Ramos, PRD **111**, 114013 (2025)
- S. W. Liu and J. J. Xie, Chin. Phys. Lett. **43**, 050202 (2026)
- P. P. Shi, M. Albaladejo, F. K. Guo and J. Nieves, arXiv:2608.01237 [hep-ph] ... **and many more**

Three-Body Systems of Molecular Nature

Three-hadron systems have been widely studied **within the molecular picture**.

For a review, see: A. Martinez Torres, K. P. Khemchandani, L. Roca and E. Oset, Few Body Syst. **61**, 35 (2020)

- $D\bar{D}K$: T. W. Wu, M. Z. Liu and L. S. Geng, PRD **103**, L031501 (2021),
  X. Wei, Q. H. Shen and J. J. Xie, EPJC **82**, 718 (2022)
- $D^*D^*D^*$: S. Q. Luo, T. W. Wu, M. Z. Liu, L. S. Geng and X. Liu, PRD **105**, 074033 (2022),
  M. Bayar, A. Martinez Torres, K. P. Khemchandani, R. Molina and E. Oset, EPJC **83**, 46 (2023)
- $\bar{K}B^*B^*$: M. P. Valderrama, PRD **98**, 014022 (2018)
- $\bar{K}^*D^*D^*$: N. Ikeno, M. Bayar and E. Oset, PRD **107**, 034006 (2023)
- DND^*: V. Montesinos, J. Song, W. H. Liang, E. Oset, J. Nieves and M. Albaladejo, PRD **110**, 054043 (2024)
- ... **and many more**

Methods widely used to study few-body bound states:

- Variational method (Gaussian expansion method)
- Fixed Center Approximation (FCA) to the Faddeev equations

$\Rightarrow$ The two approaches give consistent results, e.g. for $D\bar{D}K$ and $D^*D^*D^*$

First Calculation of a Particle–Molecule CF Using the FCA: $p\, f_1(1285)$

P. Encarnación, A. Feijoo, and E. Oset, Phys. Rev. D **111**, 114023 (2025); PRD**113**, L111502 (2026).

- $f_1(1285)$ is dynamically generated from $K^*\bar{K}$ and $\bar{K}^*K$ with $I = 0$
- The $p\, f_1(1285)$ CF was calculated using the FCA to the Faddeev equations
- A bound state was found about 40 MeV below threshold, with $\Gamma \sim 70$ MeV

An experimental analysis has also been reported by the ALICE Collaboration.

Open issue: elastic unitarity

- Elastic unitarity is essential for a reliable CF and for extracting the scattering parameters $(a,\, r_0)$.
- The standard FCA does not satisfy elastic unitarity in principle.
- In PRD **111**, the amplitude was corrected phenomenologically by $T_{\mathrm{FCA}} \to 1.5\, T_{\mathrm{FCA}}$, but the underlying problem remained unresolved.

In our work, we provide a general framework that respects elastic unitarity exactly and apply it to $n + \bar{D}^*_{s0}(2317)$

Our study: $n\,\bar{D}^*_{s0}(2317)$

$D^*_{s0}(2317)$: dynamically generated from DK $(I = 0)$

- Bound by $\sim$42 MeV below $D^0 K^+$ threshold
- The DK probability is about 72% (from lattice-data analysis)
- The natural width is very small: $\Gamma < 3.8$ MeV, due to isospin violation

$\Rightarrow$ Well-established as (mostly) a DK **molecular state** — but its nature is still debated

Why choose $n\bar{D}^*_{s0}(2317)$ instead of $pD^*_{s0}(2317)$?

- no Coulomb interaction $\rightarrow$ simpler formalism
- $\bar{K}n$ interaction is attractive and generates the $\Lambda(1405)$

$\Rightarrow$ A possible bound state of $n\bar{D}^*_{s0}$ may be formed

We study the $n\bar{D}^*_{s0}$ interaction and its correlation function.

Outline of My Talk

- Standard FCA and its unitarity problem
- Improved FCA formalism enforcing **elastic unitarity** near threshold
- Application: $n\,\bar{D}^*_{s0}(2317)$ — resonance, scattering parameters, and correlation function

Fixed Center Approximation (FCA): Setup

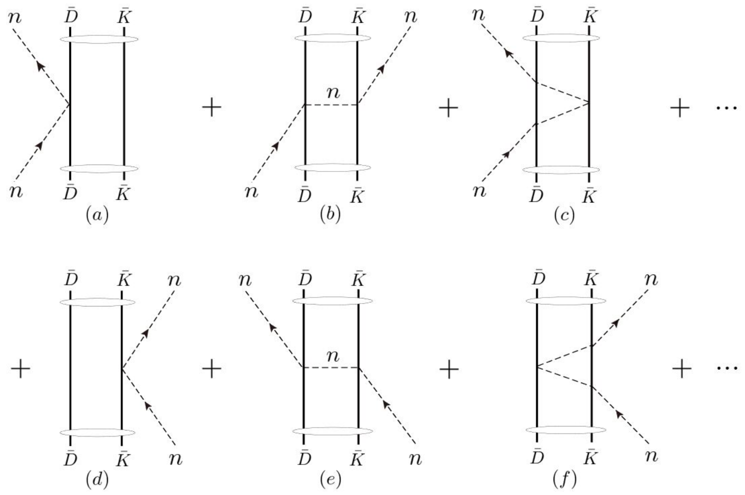

- $(\bar{D}\bar{K})_{I=0}$: **cluster**, $\bar{D}_{s0}^{*}(2317)$
- n: **external particle**

→ n scatters from the cluster **without modifying** its internal wave function

- Two elementary interactions:
  - t_1: $n\bar{D}$ scattering
  - t_2: $n\bar{K}$ scattering **(attractive, generates** $\Lambda(1405)$**)**
- $\tilde{G}$: neutron propagator folded with the cluster form factor

Partition Functions: T_{ij}

We introduce four **partition functions** T_{ij} $(i, j = 1, 2)$, labeled by the first and last collision particle in the cluster:

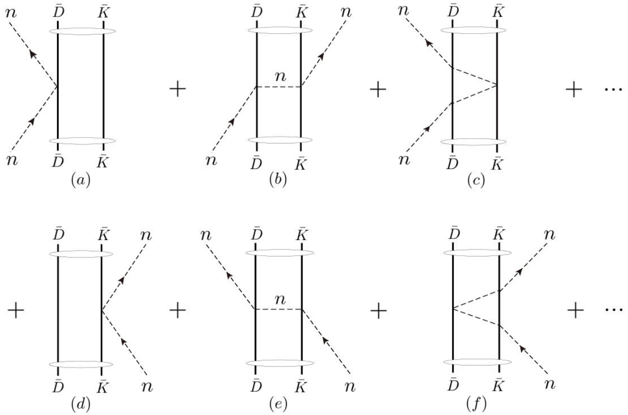

- T_{11}: starts and ends on particle 1 $(\bar{D})$
- T_{12}: starts on particle 1, ends on particle 2 $(\bar{K})$
- T_{21}: starts on particle 2, ends on particle 1
- T_{22}: starts and ends on particle 2

Each T_{ij} resums the multiple scatterings with the specified first and last collision particle.

$$
\begin{aligned}
T_{11} &= t_1 + t_1\,\tilde{G}\,T_{21},\\
T_{12} &= t_1\,\tilde{G}\,T_{22},\\
T_{21} &= t_2\,\tilde{G}\,T_{11},\\
T_{22} &= t_2 + t_2\,\tilde{G}\,T_{12}
\end{aligned}
$$

$$
T_{11} = \frac{t_1}{1 - t_1 t_2\,\tilde{G}^{\,2}}, \qquad T_{22} = \frac{t_2}{1 - t_1 t_2\,\tilde{G}^{\,2}}, \qquad T_{12} = T_{21} = \frac{t_1 t_2\,\tilde{G}}{1 - t_1 t_2\,\tilde{G}^{\,2}}.
$$

Standard FCA: Total Amplitude

The total scattering amplitude is given by

$$\widetilde{T} = \widetilde{T}_{11} + \widetilde{T}_{12} + \widetilde{T}_{21} + \widetilde{T}_{22} = \frac{\tilde{t}_1 + \tilde{t}_2 + 2\,\tilde{t}_1 \tilde{t}_2\,\tilde{G}}{1 - \tilde{t}_1 \tilde{t}_2\,\tilde{G}^{\,2}}$$

- $\widetilde{t}_1$, $\widetilde{t}_2$: rescaled $n\bar{D}$, $n\bar{K}$ amplitudes

$$t_1 \to \tilde{t}_1 = \frac{M_c}{M_{\bar{D}}}\,t_1, \quad t_2 \to \tilde{t}_2 = \frac{M_c}{M_{\bar{K}}}\,t_2,$$

- $\widetilde{G}$: the neutron propagator folded with the cluster wave function

$\to$ regularized by the cluster form factor $F_c(q)$, which encodes the DK bound-state wave function

$$\tilde{G}(\sqrt{s}) = \int \frac{d^3\boldsymbol{q}}{(2\pi)^3} \frac{M_N}{E_N(\boldsymbol{q})} \frac{1}{2\omega_c(\boldsymbol{q})} \frac{F_c(q)}{\sqrt{s} - E_N(\boldsymbol{q}) - \omega_c(\boldsymbol{q}) + i\epsilon}, \qquad F_c(q) = \frac{F(q)}{N}$$

$$F(q) = \int_{|\boldsymbol{p}|<q_{\max},\ |\boldsymbol{p}-\boldsymbol{q}|<q_{\max}} \frac{d^3\boldsymbol{p}}{(2\pi)^3} \frac{1}{M_c - \omega_{\bar{D}}(\boldsymbol{p}) - \omega_{\bar{K}}(\boldsymbol{p})} \cdot \frac{1}{M_c - \omega_{\bar{D}}(\boldsymbol{p}-\boldsymbol{q}) - \omega_{\bar{K}}(\boldsymbol{p}-\boldsymbol{q})}$$

Results within Standard FCA

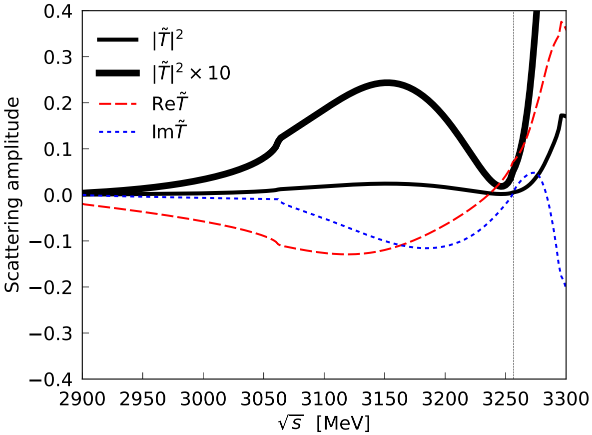

- Bound-state properties **below** threshold: maybe OK

Results within Standard FCA

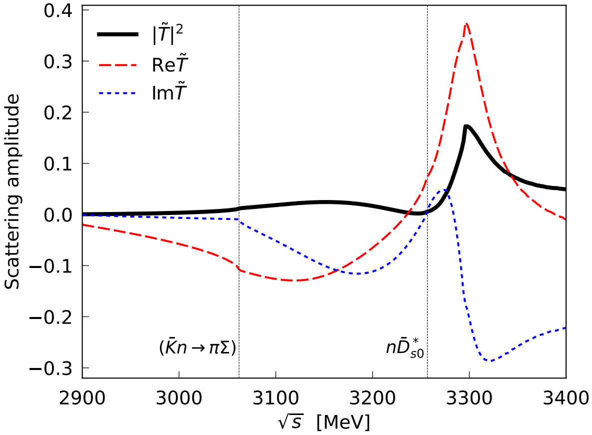

- Behaviour **above** threshold is **very strange**

→ we **cannot** use this amplitude to evaluate the correlation function or extract a, r_0

Problem: Elastic Unitarity at Threshold

In the extreme limit,

$$\tilde{t}_2 \gg \tilde{t}_1 \qquad \Longrightarrow \qquad \tilde{T} \simeq \tilde{t}_2 .$$

Near threshold, the scattering amplitude should behave as

$$\left(f^{\mathrm{QM}}\right)^{-1} \simeq -\frac{1}{a} + \frac{1}{2} r_0 q_{\mathrm{cm}}^2 - i\, q_{\mathrm{cm}}$$

q_{cm}: neutron momentum in the $n\bar{D}_{s0}^{*}(2317)$ rest frame

- The $-i\, q_{\mathrm{cm}}$ term is required by **elastic unitarity**
- The standard FCA amplitude $\tilde{T}$ does **not** reproduce this term correctly
- Consequently, the r_0 and the CF obtained from $\tilde{T}$ are not reliable

The rescue to the problem comes from nuclear physics.

What's Missing? Optical-Potential Analogy

In nuclear physics, one obtains the particle–nucleus **"optical potential"** as

$$V_{\rm opt} = t\rho \sim t_1 + t_2 + \cdots ,$$

with t the scattering matrix of the external particle with the nucleons and ρ the nuclear density. Once the optical potential is obtained, one still has to use it within the **Schrödinger equation** to obtain the full scattering amplitude.

The same logic applies to the present system:

- The standard FCA amplitude $\widetilde{T}_{\rm FCA} \sim \widetilde{t}_1 + \widetilde{t}_2 + \cdots$ can be interpreted as an optical potential

$\Rightarrow$ we still have to consider the **coherent propagation** of the neutron and the whole cluster

We include this missing propagation through new propagators G_{c1}, G_{c2}.

(the coherent n–cluster propagators — next slide)

Improved FCA: Coherent Propagation of the $n\bar{D}^*_{s0}(2317)$

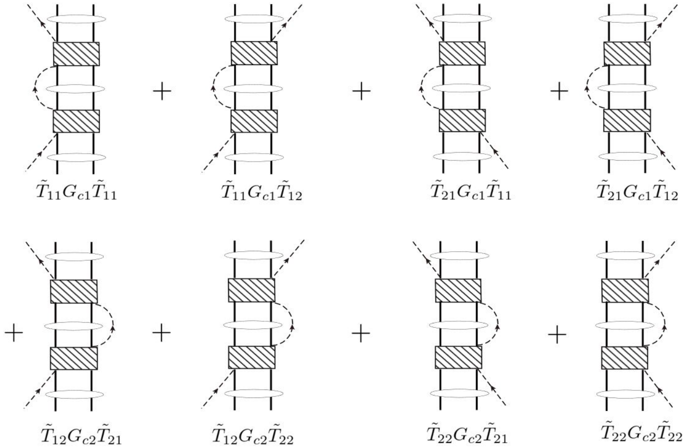

- Shaded boxes: $\widetilde{T}_{ij}$, the FCA amplitudes obtained in the previous step
- Curved lines: G_{c1} or G_{c2}, the coherent propagation of n and the whole $\bar{D}\bar{K}$ cluster

The terms shown here will be iterated to obtain the fully unitary amplitude.

Full Unitarization of the $\widetilde{T}$-matrix

The full unitarization (Lippmann–Schwinger equation) means that the kernels $\widetilde{T}_{ij}$ are iterated through multiple $n\bar{D}^*_{s0}$ intermediate steps:

$$\widetilde{T}'_{ij} = \widetilde{T}_{ij} + \widetilde{T}_{ij}\, G_c\, \widetilde{T}'_{ij}$$

which in matrix form has the solution

$$\widetilde{T}' = \left[1 - \widetilde{T}\, G_c\right]^{-1} \widetilde{T}$$

with

$$\widetilde{T}_{ij} = \begin{pmatrix} \widetilde{T}_{11} & \widetilde{T}_{12} \\ \widetilde{T}_{21} & \widetilde{T}_{22} \end{pmatrix}, \qquad G_c = \begin{pmatrix} G_{c1} & 0 \\ 0 & G_{c2} \end{pmatrix}$$

$$G_{c1}(\sqrt{s}) = \int \frac{d^3\boldsymbol{q}}{(2\pi)^3} \frac{M_N}{E_N(\boldsymbol{q})} \frac{1}{2\omega_c(\boldsymbol{q})} \frac{[F_{c1}(\boldsymbol{q})]^2}{\sqrt{s} - E_N(\boldsymbol{q}) - \omega_c(\boldsymbol{q}) + i\epsilon},$$

Finally, the total **unitarized amplitude** is

$$\widetilde{T}'_{\mathrm{sum}} = \widetilde{T}'_{11} + \widetilde{T}'_{12} + \widetilde{T}'_{21} + \widetilde{T}'_{22}$$

Checking Elastic Unitarity at Threshold

Near the $n\bar{D}_{s0}^{*}(2317)$ threshold,

$$\left[f^{\mathrm{QM}}(q_{\mathrm{cm}})\right]^{-1} \simeq -\frac{1}{a} + \frac{1}{2} r_0 q_{\mathrm{cm}}^2 - i q_{\mathrm{cm}}$$

$$\tilde{T} = -\frac{8\pi\sqrt{s}}{2M_N}\, f^{\mathrm{QM}},$$

We test elastic unitarity by checking whether $F_{\mathrm{uni}} = 1$:

$$F_{\mathrm{uni}} = \lim_{q_{\mathrm{cm}}\to 0} \frac{1}{i q_{\mathrm{cm}}} \left[\frac{8\pi\left(\sqrt{s}_{\mathrm{th}} + q_{\mathrm{cm}}^2/(2\mu)\right)}{2M_N} \left(\widetilde{T}'_{\mathrm{sum}}\right)^{-1} - \frac{8\pi\sqrt{s}_{\mathrm{th}}}{2M_N} \left(\widetilde{T}'_{\mathrm{sum}}(\sqrt{s}_{\mathrm{th}})\right)^{-1} \right]$$

We find $F_{\mathrm{uni}} = 1$ within numerical accuracy.

Once elastic unitarity is confirmed, the scattering length and effective range are obtained as

$$a = \frac{2M_N}{8\pi\sqrt{s}}\, \widetilde{T}'_{\mathrm{sum}}\Big|_{\mathrm{th}}, \qquad r_0 = \frac{1}{\mu}\left[\frac{\partial}{\partial\sqrt{s}}\left(-\frac{8\pi\sqrt{s}}{2M_N}\left(\widetilde{T}'_{\mathrm{sum}}\right)^{-1} + i\, q_{\mathrm{cm}}\right)\right]_{\mathrm{th}}$$

Resonance state below the $n\bar{D}^*_{s0}(2317)$ threshold

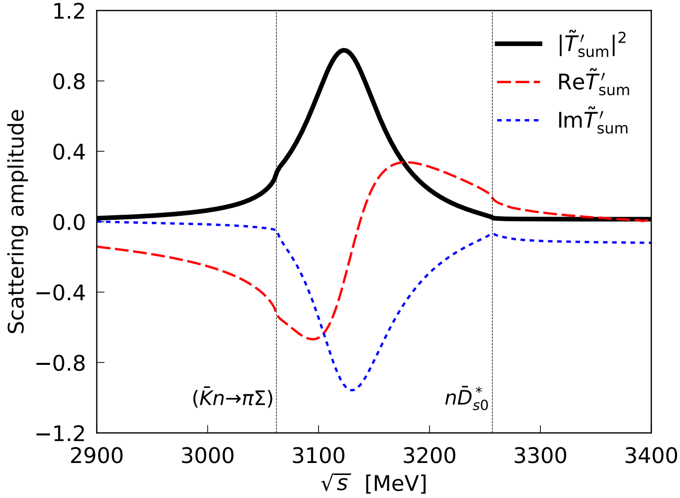

- $\tilde{T}'_{\rm sum}$ shows a Breit–Wigner-like shape below threshold
- Peak of $|\tilde{T}'_{\rm sum}|^2$:
  - binding $\sim$130 MeV below threshold
  - width $\sim$80 MeV
- The large width originates from the $\bar{K}n \to \pi\Sigma$ transition

Experimental signature: A broad $\bar{D}\pi\Sigma$ signal would support the $\bar{D}\bar{K}$ molecular nature of $\bar{D}^*_{s0}(2317)$.

The $n\,\bar{D}^*_{s0}(2317)$ Correlation Function

$$C_{n\bar{D}^*_{s0}}(p) = 1 + 4\pi \int dr\, r^2 S_{12}(r) \left\{ \left| j_0(pr) + (\widetilde{T}'_{11} + \widetilde{T}'_{21})\widetilde{G}_1 + (\widetilde{T}'_{12} + \widetilde{T}'_{22})\widetilde{G}_2 \right|^2 - j_0^2(pr) \right\}$$

- $\widetilde{T}'_{ij}$: full unitary amplitude obtained with the improved FCA
- $S_{12}(r)$: source function for the emitted $n\,\bar{D}^*_{s0}(2317)$ pair

$$S_{12}(r) = \frac{1}{\left(4\pi R^2\right)^{3/2}} \exp\left(-\frac{r^2}{4R^2}\right)$$

- $\widetilde{G}_i$: propagation factor associated with the i-th cluster constituent

→ the wave function requires the half-off-shell $\widetilde{T}'$ matrix: on-shell $\widetilde{T}'$ times the form factor $F_{ci}(q)$ inside the loop

$$\tilde{G}_i(s,r) = \int \frac{d^3\boldsymbol{q}}{(2\pi)^3} \frac{1}{2\omega_{\bar{D}_{s0}}(\boldsymbol{q})} \frac{M_N}{E_N(\boldsymbol{q})} \cdot \frac{j_0(qr)\, F_{ci}(\boldsymbol{q})}{\sqrt{s} - \omega_{\bar{D}_{s0}}(\boldsymbol{q}) - E_N(\boldsymbol{q}) + i\epsilon},$$

The $n\,\bar{D}_{s0}^*(2317)$ Correlation Function: Result

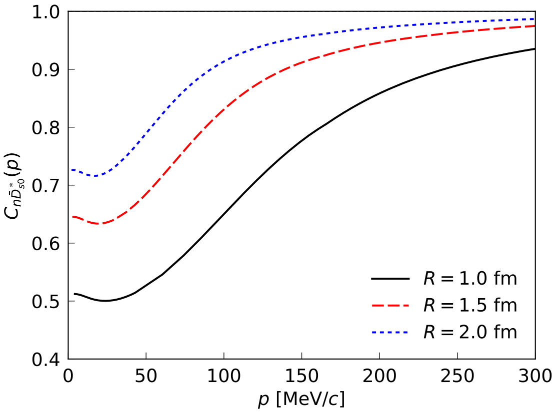

- The shape is typical of a bound or resonant state below threshold
- The shape and strength are very similar to the $p\,f_1(1285)$ correlation function

Scattering Length and Effective Range

$$a = 0.60 - i\,0.29\ \mathrm{fm},$$
$$r_0 = 1.14 - i\,0.11\ \mathrm{fm}$$

Experimentally, the correlation function can be measured by selecting a neutron and a $\bar{D}_s\pi$ pair with invariant mass around 2317 MeV.

Development and Applications of the Improved FCA

- Present work: $n\bar{D}^*_{s0}(2317)$ interaction and correlation function
  - N. Ikeno and E. Oset, Phys. Rev. D **112**, 094019 (2025)

- Subsequent development: $n\bar{D}_{s1}(2460)$ and $n\bar{D}_{s1}(2536)$
  - B. Agatão, P. Brandão, A. Martínez Torres, K. P. Khemchandani, L. M. Abreu and E. Oset, Eur. Phys. J. C **85**, 1136 (2025)

- $p\,f_1(1285)$ revisited with the improved FCA
  - P. Encarnación, A. Feijoo, and E. Oset, Phys. Rev. D **113**, L111502 (2026)

- Further applications by Jia, Song, Liang, Molina, Oset, and collaborators
  - $Kf_1(1285)$
  - $KD^*_{s0}(2317)$
  - $\pi f_1(1285)$ and $\eta f_1(1285)$
  - $K^{*+}D^{*+}K^{*+}$
  - ...
- Very recent application: πT_{cc}
  - P. Brandão, J. M. Dias and L. M. Abreu, arXiv:2608.13525 [hep-ph].

Summary

- We studied the $n\bar{D}^*_{s0}(2317)$ interaction assuming that $D^*_{s0}(2317)$ is a mostly DK molecular state.
- The standard FCA includes multiple scattering of the neutron from the two particles in the cluster, but its amplitude is not exactly unitary at threshold.
- Adding coherent n–cluster propagation restores elastic unitarity at threshold: $F_{\rm uni} = 1$
- We find a subthreshold resonance with $B \simeq 130$ MeV and $\Gamma \simeq 80$ MeV.
- The large width and the correlation function provide complementary signatures of the molecular picture.

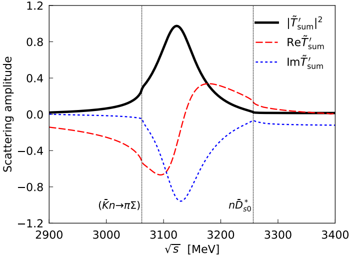

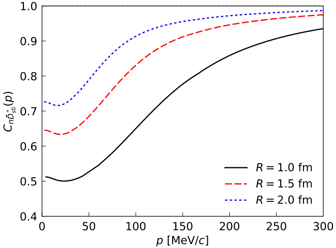

Origin of the Width and Experimental Signature

Origin of the broad width

- If $\bar{D}_{s0}^*(2317)$ were an **ordinary** (non-molecular) state:
  - a $n\bar{D}_{s0}^*(2317)$ bound state would be narrow,
  - its width would be related to $\bar{D}_{s0}^*(2317) \to \bar{D}_s\pi$, with $\Gamma < 3.8$ MeV.
- Instead, the calculated width is about 80 MeV, much larger than 3.8 MeV.
- The large width is related to the $\bar{K}n \to \pi\Sigma$ transition through the $\Lambda(1405)$ dynamics.
  - The $\pi\Sigma$ channel opens at $\sqrt{s} \simeq 3063$ MeV,
  - producing a visible kink in the amplitude.

Experimental signature

- Molecular picture: search for a broad structure in the $\bar{D}\pi\Sigma$ invariant-mass distribution.
- Ordinary-state picture: a bound state would appear in $\bar{D}_s\pi n$, with a much smaller width.

A broad $\bar{D}\pi\Sigma$ signal would support the $\bar{D}\bar{K}$ molecular nature of $\bar{D}_{s0}^*(2317)$.

Backup: Closed Form of the Unitary Amplitude

The sum of the four matrix elements can be written as

$$\widetilde{T}'_{\mathrm{sum}} = \frac{\widetilde{T}_{11} + 2\,\widetilde{T}_{12} + \widetilde{T}_{22} + \left(\widetilde{T}_{12}^{\prime 2} - \widetilde{T}_{11}\,\widetilde{T}_{22}\right)\left(G_{c1} + G_{c2}\right)}{1 - \widetilde{T}_{11}\,G_{c1} - \widetilde{T}_{22}\,G_{c2} - \left(\widetilde{T}_{12}^{\prime 2} - \widetilde{T}_{11}\,\widetilde{T}_{22}\right)G_{c1}\,G_{c2}}.$$

This is the amplitude used in the threshold test and in the CF.

Coherent propagation of the cluster

$$G_{ci}(\sqrt{s}) = \int \frac{d^3q}{(2\pi)^3} \frac{\mathcal{N}(q)[F_{ci}(q)]^2}{\sqrt{s} - E_N(q) - \omega_c(q) + i\epsilon}$$

$$\mathcal{N}(q) = \frac{M_N}{E_N(q)} \frac{1}{2\omega_c(q)}$$

$$F_{c1}(q) = F_c\left(\frac{m_2}{m_1 + m_2} q\right) ,$$

$$F_{c2}(q) = F_c\left(\frac{m_1}{m_1 + m_2} q\right) .$$

- G_{c1} and G_{c2} propagate the neutron and the whole cluster.
- F_{c1} and F_{c2} retain the internal $\bar{D}\bar{K}$ structure.
- Transitions already included in $\widetilde{t}_1 \widetilde{t}_2 \widetilde{G}$ are not counted again.

Backup: subamplitudes and invariant masses

$$s_1(n\bar{D}) = M_N^2 + (\xi m_{\bar{D}})^2 + 2\xi m_{\bar{D}} q^0,$$
$$s_2(n\bar{K}) = M_N^2 + (\xi m_{\bar{K}})^2 + 2\xi m_{\bar{K}} q^0,$$

$$q^0 = \frac{s - M_N^2 - M_c^2}{2M_c}, \qquad \xi = \frac{M_c}{M_{\bar{D}} + m_{\bar{K}}}.$$

- The invariant masses s_1 and s_2 determine the energies at which the $n\bar{D}$ and $n\bar{K}$ amplitudes are evaluated.
- The $\pi\Sigma$ channel opens through the $n\bar{K}$ subprocess.

Backup: form factors in the coherent propagators

$$F_{c1}(q) = F_c\left(\frac{m_2}{m_1 + m_2}q\right),$$

$$F_{c2}(q) = F_c\left(\frac{m_1}{m_1 + m_2}q\right).$$

- Unequal masses set different momentum arguments for the two constituents.
- The squared form factor comes from coupling the cluster at both ends.
- Cross-constituent transitions are already included in the FCA amplitude.